

A 492 GHz quasioptical SIS receiver for submillimeter astronomy

G. Engargiola

Department of Astronomy, University of Illinois, Urbana, Illinois 61801

J. Zmuidzinas

Downs Laboratory of Physics, Caltech, Pasadena, California 91125

K. Y. Lo

Department of Astronomy, University of Illinois, Urbana, Illinois 61801

(Received 31 January 1994; accepted 24 February 1994)

A 492 GHz quasioptical superconductor-insulator-superconductor (SIS) heterodyne receiver for submillimeter astronomy has been constructed with a double-sideband noise temperature of 170 ± 25 K, where the system response is an average over a 600 MHz i.f. bandwidth centered at 1.5 GHz. The excellent sensitivity is achieved through use of a planar twin-slot antenna feeding a pair of Nb-Al₂O₃-Nb junctions linked by an inductance. A main beam of $f/15$ has been measured. The performance of this receiver is comparable to that of the best 492 GHz waveguide receivers currently in operation.

I. INTRODUCTION

Because of their high sensitivity, superconductor-insulator-superconductor (SIS) tunnel junction receivers have found widespread use in millimeter-wave astronomy for nearly a decade.¹ Only within the past few years have durable, low-noise SIS mixers become available in the 450–690 GHz frequency range, largely due to improved mixer designs and the use of Nb–Al₂O₃–Nb trilayers in the manufacture of junctions.² Further efforts to improve the sensitivity of submillimeter SIS mixers continue, with the aim of eventually producing quantum-limited devices, where the mixer noise power is dominated by fluctuations in the vacuum state of the incident radiation field.

Low-noise SIS mixers generally fall into two design types, differing in how incident radiation is coupled onto the mixing element. In the waveguide mixer design, SIS mixers are suspended across waveguides into which radiation is coupled with a feedhorn; the impedance match to the mixing element is optimized with an *E*-plane tuner and a backshort.¹ In the quasioptical mixer design, the mixing elements are connected by superconducting microstrip to a broad-band planar antenna of fixed tune; the combination of a quartz hyperhemisphere and a plastic lens are used to slow the main beam of the antenna, in order to make optical matching to the telescope easier.³

Until recently, waveguide mixers have demonstrated significantly higher sensitivity than their quasioptical counterparts. However, the motivation to improve quasioptical mixers remains strong since they should be easier to produce for higher frequencies and for imaging arrays. Waveguide dimensions scale with the wavelength of operation, and the waveguide surfaces must be machined to micrometer range accuracy for frequencies above 500 GHz in order to assure low attenuation and good performance. In open-structure mixers, the elements whose sizes scale with the wavelength are easily fabricated using standard photolithographic techniques. However, quasioptical mixers still suffer from a few problems. Planar antennas have been developed which have satisfactory beam patterns (including amplitude, phase, and

cross-polarization response), but their power coupling to free space modes is still at least 30%–40% less efficient than waveguide feedhorns.^{4–7} Another potential problem is the lack of a tunable element comparable to a waveguide backshort. However, integrated fixed-tuned rf matching circuits have been developed which significantly increase the quantum efficiency and bandwidth of quasioptical mixers.⁸

In this paper, we describe the design and performance of a 492 GHz quasioptical SIS heterodyne receiver with sensitivity comparable to the best waveguide receivers currently operating at this frequency.^{9,10}

II. RECEIVER CONFIGURATION

A schematic drawing of the 492 GHz receiver is shown in Fig. 1. A 25 μm thick mylar beamsplitter mounted to the dewar injects local oscillator radiation, which is vertically polarized. A Teflon lens matches the LO to the $f/15$ beam of the receiver. Approximately 10% of the LO power (1–15 μW) is reflected into the dewar, with the remainder transmitted onto an Eccosorb termination.¹¹

The dewar is a hybrid design by Ellison.¹² An outer radiation shield at 51 K and an inner one at 15 K enclose a work surface, which is mounted to a liquid helium reservoir. The shields are cooled by a two-stage CTI 350 helium refrigerator.¹³ Radiation enters the dewar through a vacuum window made from 25 μm thick Mylar sheet. Room-temperature infrared emission is filtered from the beam with a 1.27 mm thick *z*-cut quartz disk which covers the aperture in the 51 K shield; the quartz is antireflection coated with low-density polyethylene. The aperture in the 15 K shield is open. The mixer block and a charcoal adsorption pump are clamped onto the work surface at 4.2 K, and an NRAO 1.2–1.8 GHz HEMT amplifier,¹⁴ which provides 31 dB of gain, is mounted to the inside of the 15 K shield.

The i.f. chain is a standard design. Stainless steel coaxial cable carries the i.f. signal from the mixer block to the cooled L-band amplifier via a Pamtech LTE 1310 K cryogenic isolator.¹⁵ The isolator, which terminates any power reflected back to the mixer from the amplifier, somewhat

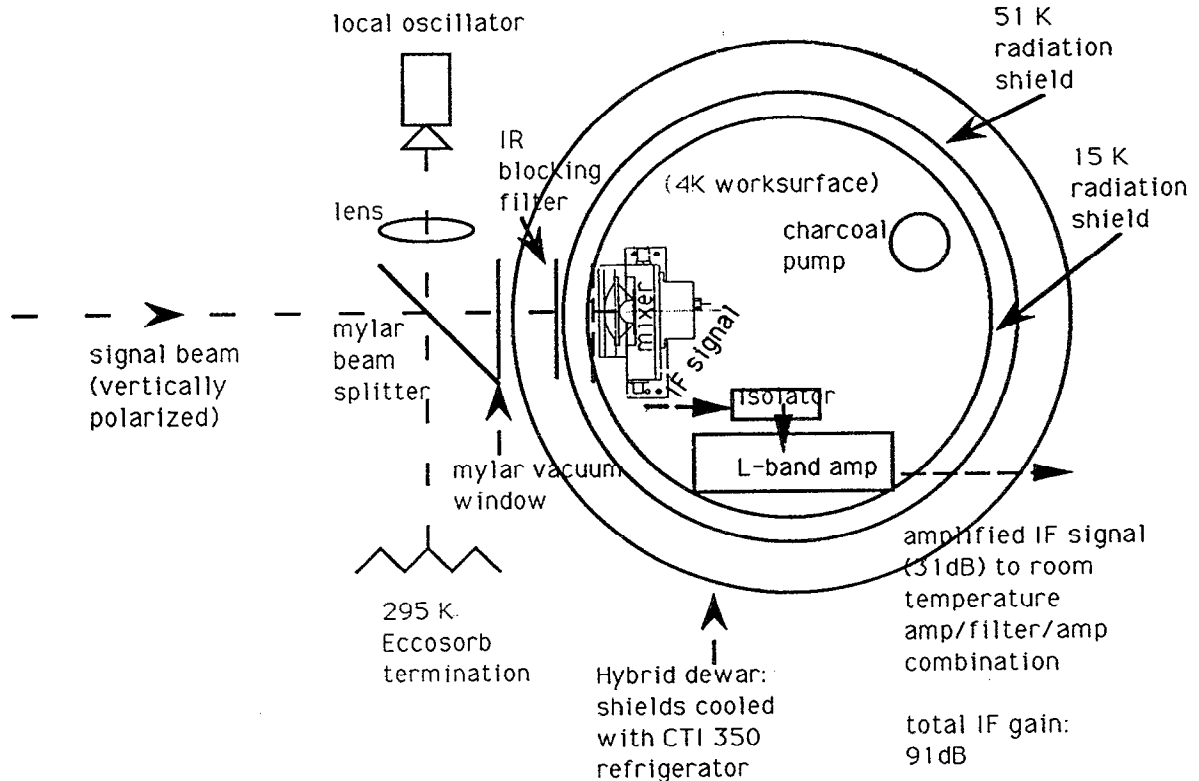


FIG. 1. A schematic drawing of the 492 GHz receiver. A Mylar beam splitter combines the LO with the signal. Microwave radiation injected into the dewar passes a Mylar pressure window and an IR blocking filter. A plastic lens and a quartz hyperhemisphere match the radiation to the planar antenna on the mixer substrate mounted inside the open structure mixer block.

improves mixer performance. The i.f. signal, after amplification at the 15 K stage, is fed into a room-temperature amplifier/filter/amplifier combination mounted to the outside of the dewar, which boosts the signal an additional 60 dB and defines a -1 dB passband of 600 MHz centered at 1.5 GHz. The shape of the i.f. passband is quite flat, varying about 1.0 dB pp; no padding is required to suppress standing waves on the ~ 3.5 ft of coaxial cable inside the dewar. For astronomical observations, the i.f. passband is upconverted from 1.5 to 2.0 GHz and analyzed with an acousto-optical spectrometer; for laboratory heterodyne measurements, a simple square-law detector (an HP 3331D planar doped barrier sensor)¹⁶ is used to measure total i.f. power.

The mixer design consists of a planar twin-slot antenna and a pair of $2.25 \mu\text{m}^2$ Nb-Al₂O₃-Nb junctions linked by an inductor. The mixer circuit is shown in Fig. 2. The dimensions of the antenna slots are $0.50 \lambda_0 \times 0.02 \lambda_0$ and the inter-slot spacing is $0.28 \lambda_0$, where λ_0 is the design wavelength; Ref. 5 contains detailed information about the twin-slot antenna characteristics. The mixers were fabricated at the Jet Propulsion Laboratory using optical lithography with three mask levels. The first mask defines the ground plane and twin-slot antenna, the second mask defines the junction area, and the third mask defines the wiring layer (contact pads, transmission lines, and radial stubs). The parallel junction circuit is fed at opposite ends by the two slots, which are 180° out of phase. Since the junctions are driven antisymmetrically, an effective rf ground occurs midway between them at the center of the inductor. The inductance L is there-

fore chosen so that $L/2$ resonates with the geometric capacitance of a single junction at 492 GHz. The junctions ($\sim 8 \Omega$) are matched to the antennas ($\sim 35 \Omega$) with two-section quarter-wave transformers; the transformers are rf coupled to the slots with radial stubs. Simulations with Touchstone¹⁷ and measurements with a Fourier transform spectrometer

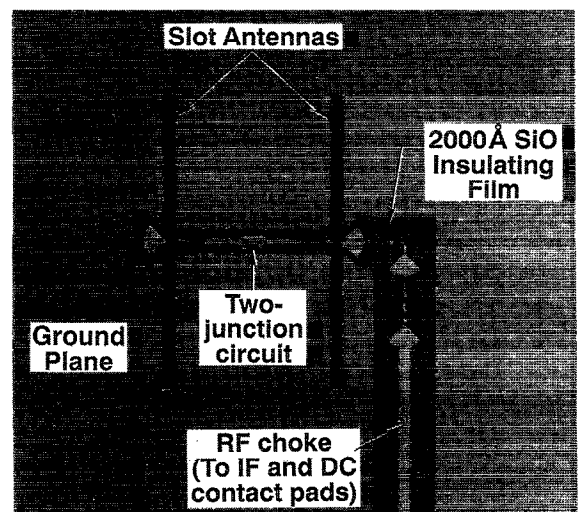
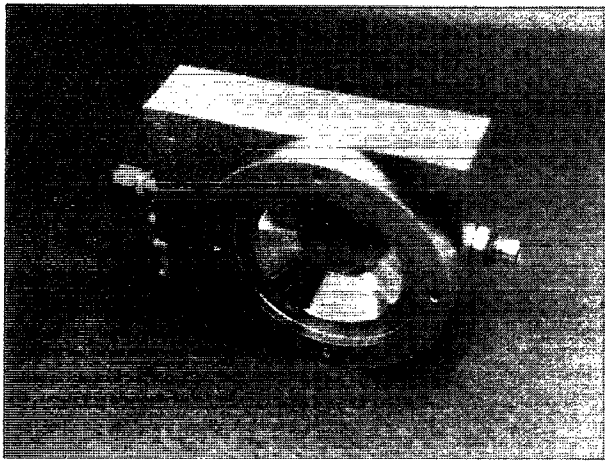
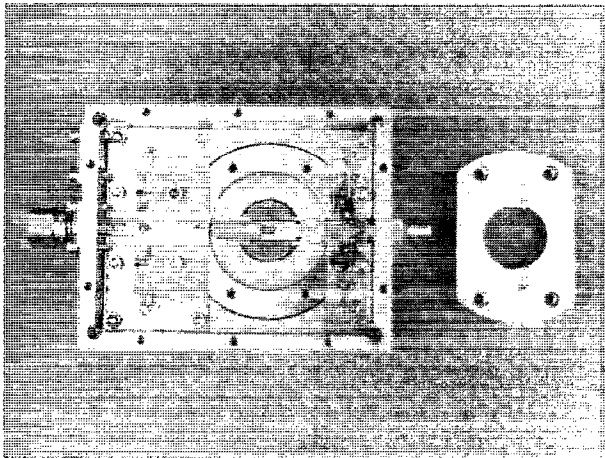


FIG. 2. A photograph of the slot antenna mixer. The twin-slot antenna antisymmetrically feeds the two-junction array with a pair of two-section quarter-wave transformers.



(a)



(b)

FIG. 3. Two views of the quasioptical mixer block: (a) Front view, with the polyethylene lens removed, showing the quartz hyperhemispheric lens—the hyperhemisphere slows the $f/0.5$ beam of the twin-slot antenna to $f/1.0$. (b) Back view, with the electromagnet mounting plate removed. The mixer on a quartz mounting disk, the $15\ \Omega$ stripline, and discrete components of the mixer block circuit are visible. The dc lines, which are protected by $1\ \text{K}$ series resistors and rf shorting capacitors, are attached to a Microtech connector (see Ref. 22). The bias tee and i.f. matching circuit are fabricated on a RT/Duroid 60160 circuit board; the i.f. signal is brought out of the mixer block with an SMA connector.

demonstrate that this mixer design has a rf $-3\ \text{dB}$ bandwidth of $\geq 200\ \text{GHz}$.

Both front and inside views of the mixer block are shown in Fig. 3. In Fig. 3(a), the HDPE plano-convex lens which attaches to the front of the mixer block has been removed to show a quartz hyperhemisphere and the mixer substrate, which is visible behind it. The hyperhemisphere transforms the $f/0.5$ main beam of the planar antenna to approximately $f/1.0$, and the plastic lens further slows the beam to about $f/15$. The beam pattern of the receiver, which was measured by scanning a small $600\ \text{K}$ blackbody source across the aperture, is shown in Fig. 4; the $-10\ \text{dB}$ width of the beam is 3.0° . The large $f/\#$ is convenient for optical matching to a telescope beam: the aperture coupling is less sensitive to small offsets relative to the beam axis, making it easier to align the LO and obtain the best coupling efficiency. Total optical losses, including vacuum window ($0.32\ \text{dB}$), IR blocking filter ($0.22\ \text{dB}$), plastic lens ($0.41\ \text{dB}$), hyperhemi-

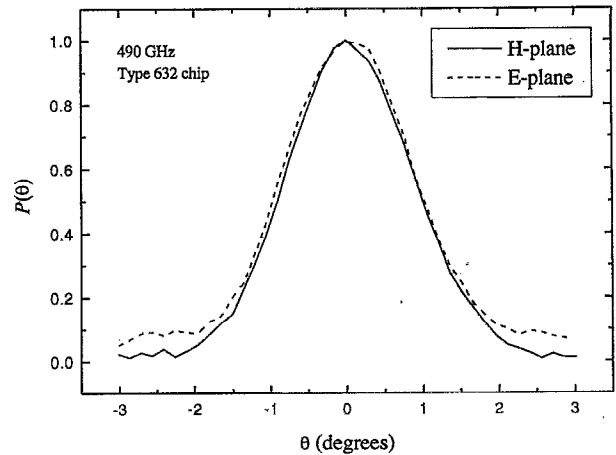


FIG. 4. The antenna profile of the quasioptical receiver measured along the H -plane (solid line) and E -plane (dash line). The $-10\ \text{dB}$ width of the main beam is 3.0° along both directions. Sidelobes are slightly higher along the E -plane.

sphere ($0.66\ \text{dB}$), and antenna efficiency ($1.55\ \text{dB}$), sum to $3.16\ \text{dB}$; these contribute to the total conversion loss of the mixer, which is discussed in the next section. In Fig. 3(b), the magnet assembly and mounting plate have been removed to show the mixer block interior. The i.f. matching network and mixer bias tee are fabricated on pieces of RT/Duroid 6010 circuit board¹⁸ attached to the inside front of the block. The mixer is wire bonded to a small $15\ \Omega$ stripline fabricated on a $0.25\ \text{mm}$ thick piece of crystal quartz. The stripline, which feeds the i.f. matching network and carries the dc bias voltage, is epoxied to the quartz mixer mounting disk, on which a ground plane has been patterned.

The mixer block incorporates an electromagnet which suppresses Josephson tunneling currents in the mixer. The magnet coil, which is made from $0.1\ \text{mm}$ Nb-Cu wire wound onto a cylindrical steel core, is mounted on the back plate of the mixer block. Steel yoke pieces attached to the ends of the coil penetrate the mixer block and make contact at right angles with flat pole pieces, which are clamped on opposite sides of the mixer mounting disk. The tapered ends of the pole pieces, which are suspended $\sim 1.0\ \text{mm}$ over the mounting disk, closely bracket the mixer. The concentrated field which develops between the pole tips adequately suppresses the Josephson effect when a few $\times 10\ \text{mA}$ is applied to the superconducting magnet windings.

III. RECEIVER PERFORMANCE

All heterodyne tests of the receiver were performed with a free running local oscillator nominally set to $492\ \text{GHz}$. The local oscillator consists of a continuously tunable $88\text{--}100\ \text{GHz}$ Gunn oscillator¹⁹ and a frequency quintupler.²⁰ The SIS mixer current as a function of dc bias voltage is shown in Fig. 5 for three different conditions: (a) with no local oscillator or magnetic field applied; (b) with a small applied magnetic field, inadequate to suppress the Josephson tunneling currents completely, but enough to enhance a rf tuning structure resonance; (c) with the Josephson currents completely suppressed by the magnetic field and the junctions pumped

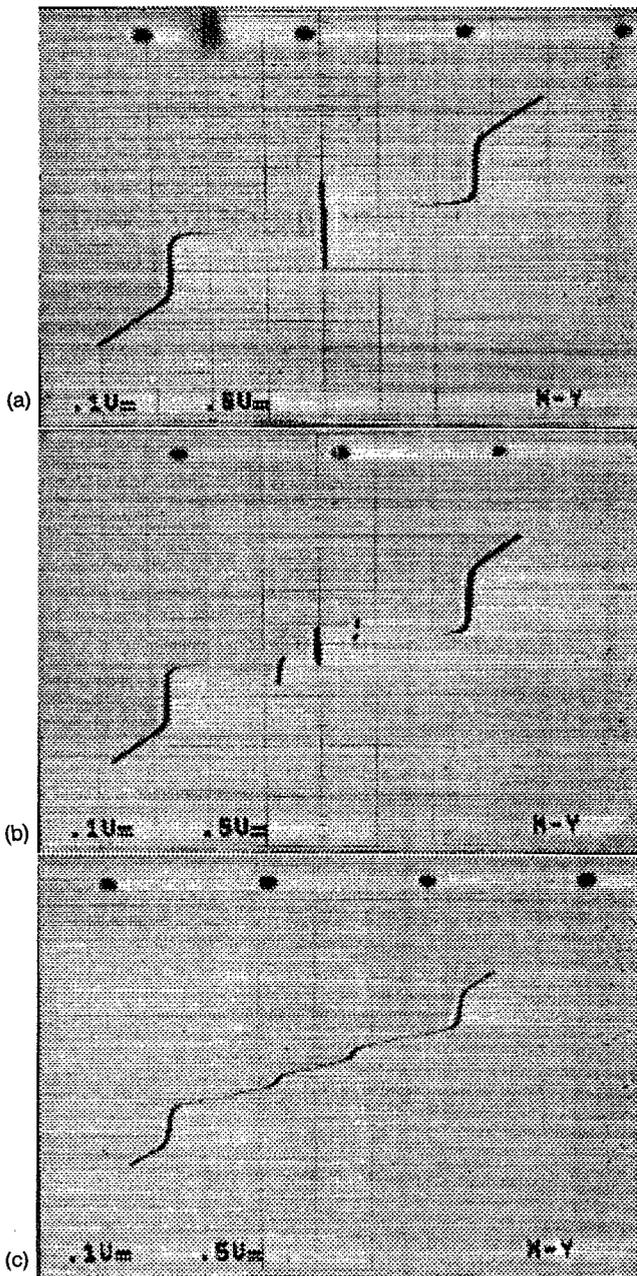


FIG. 5. Oscilloscope traces of current vs bias voltage for the mixer under three conditions: (a) With no LO or magnetic field applied—Josephson tunneling currents at zero bias voltage and a sharp nonlinearity at 2.8 mV are apparent. (b) With a small magnetic field applied—a resonance between the complex out-of-band impedance of the antenna and the two-junction tuning circuit appears at 0.7 mV (see text). (c) With the Josephson effect suppressed by a magnetic field and the mixer fully pumped at 492 GHz—the first photon step below the gap voltage is clearly visible.

by the local oscillator. Figure 5(a) shows the exceptional nonlinear characteristics of Nb–Al₂O₃–Nb junctions. The transition from superconducting to normal state occurs over a narrow bias voltage interval (~0.2 mV) centered at 2.8 mV. The conductance below the gap voltage appears to be somewhat high (~0.08 when normalized by the normal-state conductance), with a leakage current of 47 μA at 2.0 mV. Nonetheless, this device should show excellent quantum mixing, in accordance with theory.²¹ In Fig. 5(b), a resonance



FIG. 6. i.f. power as a function of voltage for hot (295 K) and cold (80 K) loads placed at the receiver input. Also shown: i.f. power when LO turned off; zero level of square-law detector.

appears on the *I-V* curve at 0.7 mV, driven by ac Josephson currents of frequency 340 GHz, where the complex out-of-band impedance of the planar antenna resonates with the impedance of the two-junction tuning circuit. Circuit simulations predict an analogous resonance. In Fig. 5(c), the device is fully pumped and the Josephson currents are visibly suppressed. The characteristic steplike structure in the *I-V* curve is due to photon-assisted tunneling of quasiparticles (electrons). The width of the photon step (2.0 mV) corresponds to the electric potential ($h\nu/e$) of a 492 GHz photon. The SIS current at the bias voltage corresponding to the middle of the first photon step is the sum of contributions from both leakage and photon-assisted tunneling.

Figure 6 shows an oscilloscope trace of the i.f. signal power as a function of bias voltage for three situations: the receiver with a 290 K blackbody at the input (top curve), the receiver with an 80 K blackbody at the input (middle curve), and the receiver without LO power (bottom curve). A magnetic field has been applied to suppress Cooper pair tunneling. The straight line at the bottom indicates the zero level of the square-law detector. The broad feature in the i.f. power curve on the first photon step arises from quasiparticle mixing. The jagged features appearing at bias voltages less than 1.5 mV are noise power resulting from chaotic Josephson currents. It is clear that the receiver sensitivity varies with bias voltage across the first photon step. A measure of this sensitivity is the *Y*-factor, which is the ratio of i.f. power for hot/cold thermal loads. A *Y*-factor can be converted to a noise temperature with the standard expression,

$$T_{\text{rec}} = [T_h - Y * T_c] / (Y - 1). \quad (1)$$

The receiver is most sensitive when biased at a voltage where the i.f. power is roughly a maximum. The best noise temperatures (150–200 K) were obtained for the interval of voltages between the two i.f. subpeaks at 1.7 and 2.1 mV. Within this interval, the most stable bias voltage settings cor-

respond to extremum in the i.f. power; at these settings, Y -factors are highly repeatable, with less than 0.1 dB variations over several hours.

Tuning to obtain maximum sensitivity requires the adjustment of three parameters—the bias voltage, the local oscillator power, and the applied magnetic field—all of which are coupled, since the linked junction pair in the mixer forms a superconducting quantum interface device (SQUID) loop. Varying the bias voltage alters the SIS current, and hence slightly changes the magnetic flux in the SQUID loop. Likewise, varying the applied LO power will alter the SIS current with the same result. The SQUID effect is observed in the Josephson branch of the I - V curve as a series of oscillations which accompany changes in the applied B -field. The SQUID effect is also evident by the varying number and amplitude of jagged noise features appearing in the i.f. power curve.

The procedure for tuning is iterative. First, the magnet current is slowly increased from zero to the lowest level (~ 40 mA) where the Josephson current branch of the IV curve nearly vanishes for some local SQUID minimum; care should be taken not to apply too high a magnetic field, which will suppress superconductivity in the mixer. The LO is applied and the power is adjusted until the heights of the two subpeaks on the i.f. power curve are about equal; this empirically gives the best sensitivity and conversion loss. The bias voltage is then fixed and the Y -factor is measured. Further small adjustments in the magnet current, bias voltage, and LO power may be necessary in order to optimize the Y -factor and to minimize interference from the Josephson effect.

Shot noise from an unpumped mixer can be used to evaluate the noise contribution from the i.f. chain referred to the input of the cooled amplifier.¹ When biased above the gap voltage, the mixer emits power in a bandwidth $\Delta\nu$ into the cooled amplifier input:

$$P_{\text{SIS}} = eI_{\text{bias}}R_N\Delta\nu. \quad (2)$$

The output voltage of the square-law detector V_{det} is linearly proportional to the net i.f. noise power:

$$V_{\text{det}} = a_{\text{calib}}(T_{\text{i.f.}} + P_{\text{SIS}}/k_B\Delta\nu), \quad (3)$$

where $T_{\text{i.f.}}$ is the noise power of the i.f. chain referred to its input. By measuring V_{det} for two bias settings and using Eqs. (2) and (3), we solve for a_{calib} , the calibration constant of the square-law detector output, and $T_{\text{i.f.}}$. The value we found for $T_{\text{i.f.}}$, the combined noise due to all i.f. components and cables, is 12 K. With a_{calib} and $T_{\text{i.f.}}$ known, the mixer conversion loss can be derived from the hot/cold load tests. The power from the pumped mixer into the i.f. amplifier is

$$P_{\text{SIS}} = k_B[T_{\text{mix}} + T_{\text{load}}]\Delta\nu/L, \quad (4)$$

where L is the mixer conversion loss, T_{mix} is the combined noise temperature of the mixer and dewar optics, referred to the rf input, and T_{load} is the temperature of the blackbody load. Using Eqs. (3) and (4) evaluated for 295 and 80 K loads, we solve for L and T_{mix} . The overall noise temperature of the receiver is related to T_{mix} and $T_{\text{i.f.}}$ by

$$T_{\text{rec}} = T_{\text{mix}} + LT_{\text{i.f.}} \approx 170 \text{ K}. \quad (5)$$

TABLE I. Comparison of 492 GHz receivers: Quasioptical (QO) and waveguide (WG).

Parameter	QO ₁	QO ₂	WG ₁	WG ₂
T_{rec} (K)	170	420	176	120
T_{mix} (K)	128	310	130	102
L (dB)	5.4	10.4	8.3	5.7
$T_{\text{i.f.}}$ (K)	12	10	6.8	4.8
R_n (Ω)	4.2	9.0	84	100
Ref.	This paper	5	9	10

Note that L includes the loss due to the rf optics.

Table I lists double side-band noise temperatures and conversion losses for several 492 GHz SIS receivers which have been recently constructed.^{5,9,10} These include the receiver described in this paper (QO₁), an earlier generation quasioptical receiver (QO₂), and two low-noise 492 GHz waveguide systems (WG₁ and WG₂).

The earlier generation quasioptical receiver, QO₂, has a DSB receiver temperature more than twice that of QO₁. Both receivers have similar rf optics, including a planar twin-slot antenna. However, the QO₂ mixer has a single untuned 2.25 μm^2 junction coupled to the antenna with a tapered transmission line. The measured conversion loss of QO₁ is nearly three times less than that of QO₂, in agreement with our calculations, and demonstrating the improvement possible with an integrated matching circuit.

A comparison of QO₁ to the waveguide receivers shows that it has comparable sensitivity, with a somewhat lower conversion loss. A reduction in the effective noise temperature of the i.f. chain in QO₁ seems possible, given the lower values achieved for WG₁ and WG₂.

IV. DISCUSSION

In this paper we have described the design and performance of a 492 GHz quasioptical SIS receiver with an integral twin-slot planar antenna matched to a pair of SIS junctions linked by an inductance. Our results show that quasioptical receivers can be constructed with conversion losses and noise temperatures comparable to those of the most sensitive waveguide receivers currently in operation.

Scans across the dewar aperture with a blackbody source indicate a main beam of $f/15$. Heterodyne tests show a DSB noise temperature of 170 K. Combined with measurements of shot noise from the unpumped mixer, these results imply a conversion loss of 5.4 dB, a mixer temperature of 128 K, and an i.f. chain noise temperature of 12 K.

ACKNOWLEDGMENTS

We wish to thank Rick LeDuc for the fabrication of the SIS junctions, Ed Sutton for helpful discussions and Jacob Kooi, David Miller, and Greg Wright for assistance with laboratory measurements. G. Engargiola and K. Y. Lo acknowledge partial support by the National Science Foundation under a cooperative agreement with the Center for Astrophysical Research in Antarctica, grant number NSF DPP

89-20223. J. Zmuidzinis acknowledges partial support by NASA (NAGW-107 and NAG2-744), NASA/JPL, and a NSF Presidential Young Investigator grant.

- ¹D. P. Woody, R. E. Miller, and M. J. Wengler, *IEEE Trans. Microwave Theory Tech.* **33**, 90 (1985).
- ²A. W. Lichtenberger, C. P. McClay, R. J. Mattauch, and M. J. Feldman, *IEEE Trans. Magn.* **25**, 1247 (1989).
- ³Thomas H. Buttgenbach, *IEEE Trans. Microwave Theory Tech.* **41**, 1750 (1993).
- ⁴A. Eckart, A. I. Harris, and R. Woheben, *Int. J. Infrared Millimeter Waves* **9**, 505 (1988).
- ⁵J. Zmuidzinis and H. G. LeDuc, *IEEE Trans. Microwave Theory Tech.* **40**, 1797 (1992).
- ⁶M. J. Wengler, D. P. Woody, R. E. Miller, and T. G. Phillips, *Int. J. Infrared Millimeter Waves* **6**, 697 (1985).
- ⁷T. H. Buttgenbach, H. G. LeDuc, P. D. Maker, and T. G. Phillips, *IEEE Trans. Appl. Superconductivity* **2**, 165 (1992).
- ⁸J. Zmuidzinis, H. G. Le Duc, J. A. Stern, and S. R. Cypher, *IEEE Trans. Microwave Theory Tech.* **42**, 698 (1994).
- ⁹C. K. Walker, J. W. Kooi, M. Chan, H. G. LeDuc, P. L. Schaeffer, J. E. Carlstrom, and T. G. Phillips, *Int. J. Infrared Millimeter Waves* **13**, 785 (1992).
- ¹⁰G. de Lange, C. E. Honingh, M. M. T. M. Dierichs, H. H. A. Schaeffer, J. Kuipers, R. A. Panhuizen, T. M. Klapwijk, H. van de Stadt, M. W. M. de Graauw, E. Armandillo, "Quantum limited responsivity of a Nb/Al₂O₃/Nb SIS waveguide mixer at 460 GHz," *Proceedings of the Fourth International Symposium Space Terahertz Technology (UCLA)*, 1993.
- ¹¹Eccosorb, Emerson & Cumming, W. R. Grace & Co., Canton, Massachusetts 02021.
- ¹²B. N. Ellison, *Cryogenics* **28**, 779 (1988).
- ¹³CTI 350 helium refrigerator, CTI-Cryogenics, Helix Technology Corporation, 9 Hampshire St., Mansfield, Massachusetts 02048.
- ¹⁴1.2–1.8 GHz HEMT amplifier, National Radio Astronomy Observatory, Charlottesville, Virginia 22903.
- ¹⁵Pamtech LTE 1310 K cryogenic isolator, Passive Microwave Technologies, 1151 Avenida Acaso, Carmarillo, California 93010.
- ¹⁶HP 33331D Coaxial rf & Microwave Detector, Hewlett-Packard Co., 5201 Tollview Dr., Rolling Meadows, Illinois 60008.
- ¹⁷Touchstone, EEsof, Inc., 5795 Lindero Canyon Rd., Westlake Village, California 91362.
- ¹⁸RT/Duroid 6010, Rogers Corp., 100 S. Roosevelt Ave., Chandler, Arizona 85226.
- ¹⁹Continuously tunable 88–100 GHz Gunn oscillator, J. E. Carlstrom Co., 262 S. Greenwood Ave., Pasadena, California 91107.
- ²⁰Microwave frequency quintupler, Radiometer Physics, Bergerwiesenstrasse 15, 5309 Meckenheim, Köln, Germany.
- ²¹J. R. Tucker and M. J. Feldman, *Rev. Mod. Phys.* **57**, 1055 (1985).
- ²²Microtech, Inc., 1420 Conchesteer Hwy., Boothwyn, Pennsylvania 19061.